Available online at www.sciencedirect.com
ScienceDirect
International Journal of Thermal Sciences 48 (2009) 964–974
International Journal of Thermal Sciences
www.elsevier.com/locate/ijts

Study of thawing behavior of liquid metal used as computer chip coolant

Kun Quan Ma, Jing Liu *, Shi Hai Xiang, Kai Wang Xie, Yi Xin Zhou

Chinese Academy of Sciences, Technical Institute of Physics and Chemistry, P.O. Box 2711, Beijing 100190, P.R. China

Received 26 October 2007; received in revised form 5 August 2008; accepted 5 August 2008

Available online 12 September 2008

Abstract

Liquid metal has recently been identified as an excellent coolant for the thermal management of computer chip. However, in an extremely low temperature environment, the liquid metals may subject to solidification due to local freezing, which may possibly cause failure of their flowing role in transferring heat away. To resolve this potential difficulty, we proposed here to quickly melt the frozen coolant by implanting in advance a wire heater into the liquid metal. A theoretical model was set up to characterize such phase change heat transfer problem through introduction of moving heat source principle. And a closed form analytical solution was obtained using Green's function under several typical boundary conditions. Meanwhile, proof-of-concept experiments were also performed in a refrigerator closet to validate the theoretical prediction. Both theoretical results and experimental measurements reveal that, the frozen metal can be successfully thawed within several dozens of seconds. This would guarantee a quick start and highly safe running of liquid metal for computer chip cooling.

Keywords: Chip cooling; Liquid metal coolant; Thawing; Frozen liquid; Phase change heat transfer; Low-melting metal or alloy; Thermal management; Moving heat source; Green's function

1. Introduction

In recent years, the continuous increase of extraordinary large amount of heat and especially high heat flux generated in computer chip made the thermal management a major serious concern throughout the world. To address such tough issue, Liu and Zhou proposed to use liquid metal or its alloy as the cooling fluid for a high performance thermal management of computer chip [1]. The later work by Miner and Ghoshal [2], Silverman et al. [3] further strongly support this endeavor. It can be noted that, the liquid metal has long historically been applied in the nuclear reactor cooling and many high melting point metals such as Na or K have been intensively investigated. However, adoption of liquid metal with melting point around room temperature as computer chip coolant was realized until recently. The liquid metal cooling arouse people's interests in computer world because the thermal conductivity of a metal is much higher than that of ordinary coolants such as water, oil or more organic fluids. Further, the liquid metal can flow like water and therefore tremendous heat can be transferred away and dissipated via liquid metal convection. Andreev et al. [4] investigated the molten metal channel flow under the influence of a non-uniform magnetic field experimentally. Baird and Mohseni [5,6] presented theoretical and numerical results describing digitized heat transfer (DHT), a newly developing active thermal management technique. DHT coolants, in their papers, included liquid metals and alloys. A major advantage of liquid metal coolant lies in its ability to be pumped efficiently with a silent, vibration-free, low energy consumption rate, non-moving and compact magnetofluiddynamic (MFD) pump due to the high electric conductivity [1,2]. This offers a unique solution to cooling high density power sources and quickly spreading heat away. Ma and Liu [7] even realized a liquid metal cooling device for the thermal management of computer chip without costing external energy but the waste heat generated by the computer chip. Besides, the other driving methods such as electrohydrodynamics (EHD) micro pump [8], electrowetting pump [9,10] and peristaltic pump [11] were also proved flexible for the implementation of this promising cooling strategy. Further, the recently proposed nano liquid metal [12] may serve as an even more conductive coolant in the electronics

* Corresponding author. Tel.: +86 10 82543765; fax: +86 10 82543767.
E-mail address: jliu@cl.cryo.ac.cn (J. Liu).

1290-0729/$ – see front matter
doi:10.1016/j.ijthermalsci.2008.08.005

Nomenclature

T	temperature of solid metal ..... °C	$R(\beta, r)$	elementary solution
T_m	melting point of metal ..... °C	$R_0(\beta, r)$	eigenfunction
k	thermal conductivity ..... W/(m K)	$N(\beta_m)$	norm
r	radial coordinate ..... mm	$q(r, t)$	moving heat sink
r_0	radius of wire heater ..... mm	$G(r, t\|r', t')$	Green function
R	radius of inner wall of tube ..... m	J_0, J_1, Y_0, Y_1	Bessel functions
u	velocity of liquid metal ..... m/s		
L	latent heat ..... J/kg	*Greek symbols*	
s	solid–liquid interface ..... mm	ρ	density ..... kg/m^3
Q	input power of wire heater ..... W/m	θ	temperature ..... °C
h	convective heat transfer coefficient ... W/(m^2 K)	β_m	eigenvalue
I	electric current ..... A	a	thermal diffusivity of solid metal ..... m^2/s
R_0	electric resistance ..... Ω	τ	time ..... s
L_0	length of wire heater ..... m		
q_0	heat flux ..... W/m^2	*Subscript*	
S_0	cross section area ..... m^2	s	solid state
t	time ..... s	l	liquid state
t_1	time ..... s	f	air flow

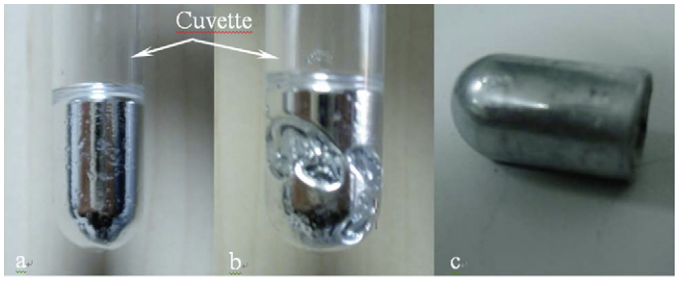

Fig. 1. Appearance of gallium for showing its freezing from liquid to solid state in a cuvette. (a) Liquid state; (b) partly frozen; (c) frozen state.

cooling, since it has a higher effective thermal conductivity. In one word, the liquid metal is becoming a very promising coolant for thermal management in a wide variety of engineering field.

Meanwhile, during the application of this new method, it was also noted that most of the freezing points of the currently available liquid metals appear higher than the environmental temperature. Therefore, such situation sometimes may cause freezing of coolant and thus stop its running in driving heat away. Although many liquid metals have a subcooling temperature, which maybe much less than their melting point [13], the subcooling state is often a unsteady condition and would easily be subjected to a small disturbance coming from outside. Fig. 1 illustrates the freezing process of liquid gallium in a cuvette. Clearly, strategies should be adopted to thaw the frozen metal as desired when one wishes to immediately switch on its flowing state.

To partially address this tough issue, one can try to use alloy with much lower melting point as coolant. For example, some of such candidates can be as $Ga_{61}In_{15}Sn_{13}Zn_1$ which has a melting point at 3 °C, and $Ga_{62}In_{25}Sn_{13}$ at 5 °C [14]. Therefore, these alloys did allow a much lower working temperature. But if the environment become colder which is often encountered during transportation of chip cooling device in winter or in a extremely low temperature environment, the liquid metal may easily subject to freezing. All in all, the solidification of liquid metal always exists as a potential hazard for its safe running as a convective coolant. This paper is dedicated to investigate the phase change problem of liquid metal fluid and establish a feasible technical approach for tackling this important issue. It is expected to be of valuable reference for designing future chip cooling device using liquid metal as coolant.

2. Theoretical model for metal thawing with central wire heater

In reality, the liquid metal was generally packaged within a tube to avoid causing potential damage to the electronics devices near the objective that requires cooling. Since the length of the objective tube is much larger than the diameter, the heat transfer process inside it can be treated as one-dimensional (1-D) problem along radial direction. Due to evident difficulty in dealing with phase change problem of the non-homogeneous material via analytical solution, all the thermal properties are treated as constant for simplicity in this study. And a fixed phase change temperature is considered, namely, the freezing point is regarded as equal to the melting point. The physical model for the liquid metal can be illustrated by Fig. 2. The wire heater is located at the central body of the solid metal at a uniform temperature T_0 within the medium. The wire heater is switched on to generate heat at time $t = 0$. For the feasibility to derive the analytically solution, the tube here was used just to hold the metal. For simplicity, it was assumed to have a high thermal conductivity and a neglectable thickness.

Then the energy conservation equations for the thawing problem of the low melting point metal in the tube can be modeled as follows:

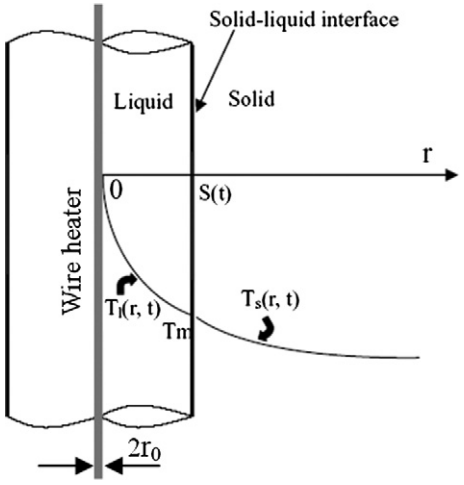

Fig. 2. Physical model for thawing process of low-melting point metal with the aid of wire heater.

Solid phase:

$$\frac{\partial T_s}{\partial t} = a_s \frac{1}{r}\frac{\partial}{\partial r}\left(r\frac{\partial T_s}{\partial r}\right), \quad \text{in } s(t) < r < R \tag{1}$$

$$T_s(r,t) = T_0, \quad t = 0,\ r > r_o \tag{2}$$

Liquid phase:

$$\frac{\partial T_l}{\partial t} + u\frac{\partial T_l}{\partial x} = a_l \frac{1}{r}\frac{\partial}{\partial r}\left(r\frac{\partial T_l}{\partial r}\right), \quad \text{in } r_o < r < s(t) \tag{3}$$

Solid–liquid moving interface:

$$T_s(r,t) = T_l(r,t) = T_m, \quad \text{at } r = s(t),\ t > 0 \tag{4}$$

Considering the energy conservation at the solid–liquid interface, one still has

$$k_s\frac{\partial T_s}{\partial r} - k_l\frac{\partial T_l}{\partial r} = \rho L\frac{ds}{dt}, \quad \text{at } r = s(t),\ t > 0 \tag{5}$$

where, T_m, α, ρ, L are the melting point temperature, diffusivity, density and latent heat of low melting point metal, respectively. The subscripts l and s denote liquid and solid state. In Eq. (3) u is the flowing velocity of metal in liquid state and $s(t)$ the solid–liquid interface. Obviously, ds/dt is the interface velocity from $r = r_0$ to $r = R$.

In Eq. (3), the flowing velocity of liquid metal in a tube u is generally small at thawing process, which can be ignored for simplicity. Meanwhile, ignoring the difference of thermal conductivity of solid and liquid state for simplicity, one has $k_s = k_l = k$. The errors thus caused can be evaluated using gallium's data in subsequent part of this paper.

Through introduction of the moving heat source concept, the above phase change problem can be equivalently transformed to a heat conduction problem with generalized purpose, i.e.

$$\frac{1}{a}\frac{\partial T}{\partial t} = \frac{1}{r}\frac{\partial}{\partial r}\left(r\frac{\partial T}{\partial r}\right) - \frac{\rho L\frac{ds}{dt}\delta[r - s(t)]}{k} \tag{6}$$

with a condition at the solid–liquid interface as

$$T(x,t) = T_m \quad \text{at } r = s(t) \tag{7}$$

where, $\delta[r - s(t)]$ is the delta function. Detail of the explanation about Eqs. (6) and (7) has been available in Ref. [15]. The minus sign in Eq. (6) is appended because the metal at solid–liquid interface absorbs the latent heat.

The absorption of heat during melting process can be treated as a moving cylindrical surface heat sink at the solid–liquid interface. With this consideration it is possible to solve the transient phase change problem by way of a transient heat conduction problem with a moving cylindrical surface heat source. The moving heat source method was originally proposed by Lightfoot for the solution of one-dimensional transient phase change problem in an infinitely large area [15]. Liu and Zhou [16] extended this approach to study the freezing and thawing process of biological skin with finite thickness. Yang [17] developed a numerical algorithm to estimate the location and the strength of two moving heat sources. Ali and Zhang [18] established a unified framework for solving heat conduction problems using the relativistic heat conduction model involving moving heat sources under various loading and boundary conditions. But none of the above efforts have been made to the solution in a cylindrical domain as will be addressed in the following section.

3. Solution to the thawing problem with moving heat source

3.1. Analytical solution

Eq. (6) can be analytically solved by Green's method. For brief, it is rewritten here as

$$\frac{1}{a}\frac{\partial T}{\partial t} = \frac{1}{r}\frac{\partial}{\partial r}\left(r\frac{\partial T}{\partial r}\right) + \frac{q(r,t)}{k} \tag{8}$$

where, $q(r,t) = -\rho L\frac{ds}{dt}\delta[r - s(t)]$.

The corresponding boundary condition for the wire heating case (Fig. 2) can be expressed as

$$-2\pi r k\frac{\partial T}{\partial r} = Q, \qquad \text{at } r = r_0 \tag{9}$$

$$-k\frac{\partial T}{\partial r} = h(T - T_f), \quad \text{at } r = R \tag{10}$$

where, Q is the heat generated by the wire heater per length. It can be depicted as follows if a current or a voltage is applied on the heater:

$$Q = I^2 R_0/L_0 \quad \text{or} \quad Q = U^2/(R_0 L_0) \tag{11}$$

where, I, U are electric current, electric voltage applied on the wire heater. R_0, L_0 are the electric resistance and length of the wire heater.

If denoting temperature difference as

$$\theta = T - T_f \tag{12}$$

one can respectively write Eqs. (2), (8)–(10) as

$$\frac{1}{a}\frac{\partial \theta}{\partial t} = \left(\frac{\partial^2\theta}{\partial r^2} + \frac{1}{r}\frac{\partial\theta}{\partial r}\right) + \frac{q(r,t)}{k} \tag{13}$$

$$-2\pi r k\frac{\partial\theta}{\partial r} = Q, \quad r = r_0 \tag{14}$$

$$-k\frac{\partial\theta}{\partial r} = h\theta, \quad r = R \tag{15}$$

$$\theta(r,0) = F(r) = T_0(r) - T_f \tag{16}$$

To determine the appropriate Green' function to the above Eqs. (13)–(16), one can solve first the homogenous version of Eqs. (13)–(16):

$$\frac{1}{a}\frac{\partial\psi}{\partial t} = \frac{\partial^2\psi}{\partial r^2} + \frac{1}{r}\frac{\partial\psi}{\partial r} \tag{17}$$

$$\frac{\partial\psi}{\partial r} = 0, \quad \text{at } r = r_0 \tag{18}$$

$$-k\frac{\partial\psi}{\partial r} = h\psi, \quad \text{at } r = R \tag{19}$$

$$\psi(r,0) = F(r), \quad t = 0 \tag{20}$$

If assuming that

$$\psi(r,t) = R(r)\Gamma(t) \tag{21}$$

Eq. (17) can be transformed as

$$\frac{1}{R}\left(\frac{d^2R}{dr^2} + \frac{1}{r}\frac{dR}{dr}\right) = \frac{1}{a\Gamma(t)}\frac{d\Gamma(t)}{dt} = -\beta^2 \tag{22}$$

Therefore, Eq. (17) using separating-variable methods has the following form:

$$\frac{d\Gamma(t)}{dt} = -a\beta^2\Gamma(t) \tag{23}$$

$$\frac{d^2R}{dr^2} + \frac{1}{r}\frac{dR}{dr} + \beta^2 R = 0 \tag{24}$$

and the elementary solution for the $\Gamma(t)$ is given as

$$\Gamma(t) = e^{-a\beta^2 t} \tag{25}$$

For the R, it is given as

$$R(\beta,r) = J_0(\beta r) \quad \text{and} \quad R(\beta,r) = Y_0(\beta r) \tag{26}$$

Under the boundary condition of (18) and (19), the eigenfunctions $R_0(\beta_m, r)$ and the norm $N(\beta_m)$ to Eq. (24) can be obtained as

$$R_0(\beta_m, r) = S_0 J_0(\beta_m r) - V_0 Y_0(\beta_m r) \tag{27}$$

$$N(\beta_m) = \frac{2}{\pi^2}\frac{B_2 J_1^2(\beta_m r_0) - V_0^2}{\beta_m^2 J_1^2(\beta_m r_0)} \tag{28}$$

where, β_m's are the positive roots of

$$\begin{aligned}&\big[-\beta_m Y_1(\beta_m R) + (h/k)Y_0(\beta_m R)\big]J_1(\beta_m r_0)\\ &\quad - \big[-\beta_m J_1(\beta_m R) + (h/k)J_0(\beta_m R)\big]Y_1(\beta_m r_0) = 0\end{aligned} \tag{29}$$

and

$$S_0 = -\beta_m Y_1(\beta_m R) + (h/k)Y_0(\beta_m R)$$

$$V_0 = -\beta_m J_1(\beta_m R) + (h/k)J_0(\beta_m R)$$

Therefore, the solution to $\psi(r,t)$ can be obtained as:

$$\psi(r,t) = \sum_{m=1}^{\infty}\frac{1}{N(\beta_m)}e^{-a\beta_m^2 t}R_0(\beta_m, r) \times \int_{r_0}^{R} r' R_0(\beta_m, r')F(r')\,dr' \tag{30}$$

Obviously, Eqs. (17)–(20) have the solution with the following form:

$$\psi(r,t) = \int_{r_0}^{R} r' G(r,t|r',\tau)|_{\tau=0} F(r')\,dr' \tag{31}$$

where, r' is Sturm–Liouville weight function.

A comparison between Eqs. (30) and (31) yields:

$$G(r,t|r',\tau)|_{\tau=0} = \sum_{m=1}^{\infty}\frac{1}{N(\beta_m)}e^{-a\beta_m^2 t}R_0(\beta_m, r)R_0(\beta_m, r') \tag{32}$$

Changing t with $(t-\tau)$, one can get the Green's function

$$G(r,t|r',\tau) = \sum_{m=1}^{\infty}\frac{1}{N(\beta_m)}e^{-a\beta_m^2 (t-\tau)}R_0(\beta_m, r)R_0(\beta_m, r') \tag{33}$$

$\theta(r,t)$ in Eqs. (13)–(16) can then be written as:

$$\begin{aligned}\theta(r,t) = {}& \int_{r_0}^{R} r' G(r,t|r',\tau)|_{\tau=0}F(r')\,dr'\\ &+ \frac{\alpha}{k}\int_0^t d\tau \int_{r_0}^{R} r' G(r,t|r',\tau)q(r',\tau)\,dr'\\ &- \alpha\int_0^t r' G(r,t|r',\tau)\frac{1}{k}f_{r'}(r,t)|_{r=r_0}\,d\tau\\ &+ \alpha\int_0^t r' G(r,t|r',\tau)\frac{1}{k}f_{r'}(r,t)|_{r'=R}\,d\tau\end{aligned} \tag{34}$$

where, $f_R(r,t) = 0$, $f_{r_0}(r,t) = -Q/2\pi r_0$.

It is to be noted that the minus sign for the term $-\alpha\int_0^t r' G(r,t|r',\tau)\frac{1}{k}f_{r'}(r,t)|_{r=r_0}\,d\tau$ is due to the fact that the outward drawn normal at the boundary surface $r = r_0$ is in the negative r direction.

Considering $q(r,t) = -\rho L\frac{ds}{dt}\delta[r - s(t)]$, Eq. (34) can finally be rewritten as

$$\begin{aligned}\theta(r,t) = {}& \sum_{m=1}^{\infty}\frac{1}{N(\beta_m)}e^{-a\beta_m^2 t}R_0(\beta_m, r)\int_{r_0}^{R} r' R_0(\beta_m, r')F(r')\,dr'\\ &- \frac{\alpha}{k}\rho L\sum_{m=1}^{\infty}\frac{1}{N(\beta_m)}R_0(\beta_m, r)\int_0^t e^{-a\beta_m^2(t-\tau)}\,d\tau\\ &\times\int_{r_0}^{R} r' R_0(\beta_m, r')\frac{ds}{dt}\delta\big[r' - s(t)\big]\,dr'\\ &+ \frac{Q\alpha}{2\pi k r_0}\sum_{m=1}^{\infty}\frac{1}{N(\beta_m)}R_0(\beta_m, r)R_0(\beta_m, r_0)\\ &\times\int_0^t e^{-a\beta_m^2(t-\tau)}\,d\tau\end{aligned} \tag{35}$$

In the above equation, one can further get the following integrating parts for solution purpose:

$$\int_{r_0}^{R} r' R_0(\beta_m, r')\,dr' = \int_{r_0}^{R} r'\big[S_0 J_0(\beta_m r') - V_0 Y_0(\beta_m r')\big]\,dr = \frac{1}{\beta_m}\big[R J_1(\beta_m R) + R Y_1(\beta_m R) - r_0 J_1(\beta_m r_0) - r_0 Y_1(\beta_m r_0)\big] \tag{36}$$

$$\int_{r_0}^{R} r' R_0(\beta_m, r')\frac{\partial s}{\partial \tau}\delta\big[r' - s(t)\big]\,dr' = \int_{r_0}^{R} r'\big(S_0 J_0(\beta_m r') - V_0 Y_0(\beta_m r')\big)\frac{ds}{dt}\delta\big[r' - s(t)\big]\,dr' \tag{37}$$

3.2. Methodology to deal with moving velocity of solid–liquid interface

It is difficult to get the unknown value of ds/dt in Eqs. (35) and (37). Liu and Zhou [16] had therefore made a simplification using $ds/dt = s/t$ when dealing with phase change in biological skin due to its small thickness. In the present study, the diameter of tube is in order of millimeter which may arouse errors if still using the method as developed before. Therefore we turn to take another more straightforward simplification which was also proved approximately true by later calculation. As is well known, in an analytical solution for semi-infinite cylinder, ds/dt has the form $ds/dt = 2a\lambda^2/s$, where λ is only a positive root of the energy balance equation at solid–liquid interface [15]. As an approximate treatment, we adopt the similar method and assume that $ds/d\tau$ has similar expression for finite cylinder as follows:

$$\frac{ds}{dt} = \frac{A}{s} \tag{38}$$

where A is a constant, which is dependent on the energy equation at solid–liquid interface.

From Eq. (38), one gets

$$s^2 = 2At + B \tag{39}$$

Regarding the condition:

$$s = 0, \quad \text{at } t = 0 \tag{40}$$

$$s = R, \quad \text{at } t = t_1 \tag{41}$$

where, t_1 is the time when all the low melting metal becomes thawed.

From Eqs. (38)–(41), considering constant numbers A and B, one gets $A = R^2/2t_1$, $B = 0$. Therefore, we have

$$\frac{ds}{dt} = \frac{R^2}{2t_1 s} \tag{42}$$

Then, Eq. (37) can be rewritten as

$$\int_{r_0}^{R} r' R_0(\beta_m, r')\frac{ds}{dt}\delta\big[r' - s(t)\big]\,dr' = r' R_0(\beta_m, r')|_{r'=s}\frac{R^2}{2st_1} = \frac{R^2}{2t_1} R_0(\beta_m, s) \tag{43}$$

Substituting Eqs. (36) and (43) into Eq. (35), one can get the final solution to the equation as:

$$\theta(r,t) = \sum_{m=1}^{\infty}\left\{\frac{[R J_1(\beta_m R) + R Y_1(\beta_m R)]e^{-a\beta_m^2 t}}{\beta_m N(\beta_m)} - \frac{[r_0 J_1(\beta_m r_0) + r_0 Y_1(\beta_m r_0)]e^{-a\beta_m^2 t}}{\beta_m N(\beta_m)}\right\} F(r) R_0(\beta_m, r) - \frac{\rho L}{2k}\sum_{m=1}^{\infty}\frac{R^2 R_0(\beta_m, r_0)(1 - e^{-a\beta_m^2 t})}{\beta_m^2 N(\beta_m) t_1} R_0(\beta_m, r) + \frac{Q}{2\pi k}\sum_{m=1}^{\infty}\frac{(1 - e^{-a\beta_m^2 t}) R_0(\beta_m, r_0)}{\beta_m^2 N(\beta_m)} R_0(\beta_m, r) \tag{44}$$

To estimate the time t_1, one can choose the time when the solid–liquid interface moves to $r = R$. At this moment, $t = t_1$. Using such condition, the time t_1 can be obtained by solving Eq. (44) under the condition $\theta(r,t) = T_m - T_f$ and $r = R$.

4. Results and discussion

In Eq. (44), one can see that the temperature distribution is dependent on the parameters such as input power of wire heater, the diameters of tube and wire heater, convective heat transfer coefficient of air, thermal conductivity and thermal diffusivity of metal. The effects of these parameters on the time requested for thawing are analyzed as follows.

4.1. Parametric studies on factors to affect the thawing time

4.1.1. Effect of wire heater power

From Fig. 3, one can see that the time for thawing metal process (gallium, for example) will be longer for the case with a lower surrounding temperature. However, the time difference is rather small throughout the whole thawing process. For example, the time needed for thawing gallium is, respectively, 267, 257 and 247 s at three different environmental temperatures when the input power of wire heater is 100 W/m. That is to say, the sensible heat is rather small compared with the latent heat, which agrees with the common sense.

4.1.2. Effect of tube diameter

The diameter of the tube has strong effect on the time needed for thawing process. As indicated before, the latent heat is much large compared with the sensible heat. The time for melting the metal gallium in different radius of the tube is shown in Fig. 4 when the wire heater power is 100, 200 W/m, respectively. Clearly, a larger diameter of the tube means that more metal needed thawing and therefore more heat and longer time is required.

Table 1
Typical thermophysical properties of gallium and parameters adopted in calculation

Items	Unit	Value
Thermal conductivity of liquid gallium	W/(m K)	29.4
Thermal conductivity of frozen gallium	W/(m K)	40.6
Thermal diffusivity of liquid gallium	m^2/s	1.83×10^{-5}
Thermal diffusivity of frozen gallium	m^2/s	1.45×10^{-5}
Latent heat of gallium	J/kg	8.01×10^4
Melting temperature of gallium	°C	29.7
Diameter of wire heater	mm	0.4
Diameter of tube	mm	8

Table 2
Time needed for thawing process with different diameters of heating wire

R_0 (mm)	0.1	0.2	0.3	0.4	0.5	0.6	0.7	0.8	0.9	1.0	2.0
100 W/m	247.4	247.4	247.4	247.3	247.3	247.2	247.2	247.1	247	246.9	245.3
200 W/m	123.4	123.4	123.4	123.3	123.3	123.2	123.2	123.1	123.1	123.1	122.3

Units: second.

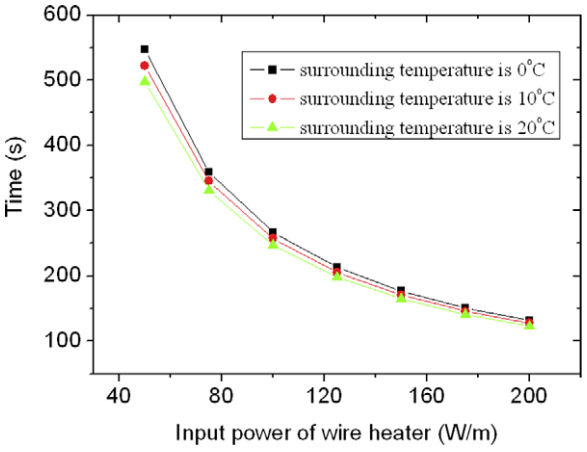

Fig. 3. The time needed for thawing gallium versus input power of wire heater with different surrounding temperature 0°, 10°, 20 °C, respectively. The diameters of tube and wire heater are 8 and 0.4 mm, respectively.

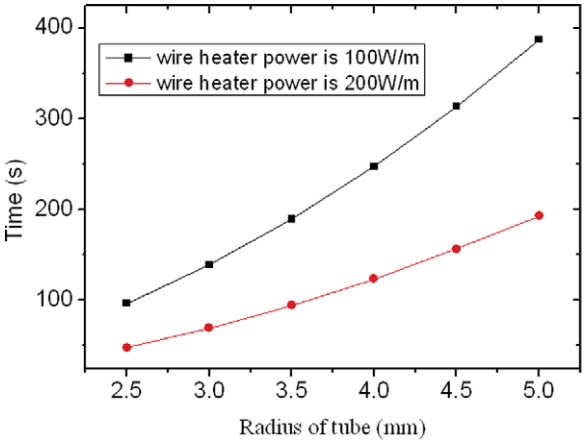

Fig. 4. Effect of tube diameter on time needed for thawing process, with diameter of heating wire as 0.2 mm, heat transfer coefficient as 5 W/(m^2 K), and surrounding temperature at 20 °C.

4.1.3. *Effect of wire heater diameter*

From Table 2, we can find that the time needed for thawing the frozen gallium stays almost unchanged with different diameters of wire heater. It is understandable because we have fixed the value of input power of the wire heater which can be appropriately regarded as a wire heater due to small diameter. In other word, if the input power of wire heater is dependent on the electrical resistance, the radius of wire heat will have effect on the time needed for the thawing process. This can be made clearer from the following relations.

According to Ohm' law:

$$R_0 = \frac{\rho L_0}{S_0} = \frac{4\rho L_0}{\pi r_0^2} \tag{45}$$

$$Q = I^2 R_0 / L_0 = \frac{4I^2\rho}{\pi r_0^2} \tag{46}$$

or

$$Q = U^2 / R_0 L_0 = \frac{U^2 \pi r_0^2}{4\rho} \tag{47}$$

where, ρ is the electric resistance of the wire heater material, L and S the length and the section cross of wire heater. I and U are electric current and voltage across the wire heater.

4.1.4. *Effect of convective heat transfer coefficient of air*

For the special case with $h = 0$ in Eq. (10), the eigenfunction and norm to equation can be changed as

$$R_0(\beta_m, r) = -J_0(\beta_m r) Y_1(\beta_m R) + J_1(\beta_m R) Y_0(\beta_m r) \tag{48}$$

$$\frac{1}{N(\beta_m)} = \frac{\pi^2}{2} \frac{\beta_m^2 J_1^2(\beta_m r_0)}{J_1^2(\beta_m r_0) - J_1^2(\beta_m R)} \tag{49}$$

where, the eigenvalue β_m's should be the roots of

$$J_1(\beta_m r_0) Y_1(\beta_m R) - J_1(\beta_m R) Y_1(\beta_m r_0) = 0 \tag{50}$$

It can be noted that β_0 is also an eigenvalue for this particular case. The corresponding eigenfunction and norm are, respectively, as follows:

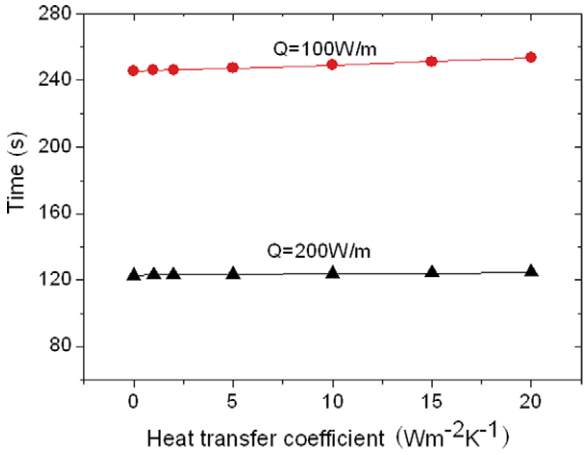

Fig. 5. Effect of heat transfer coefficient on time needed for thawing process, with diameter of heating wire as 0.4 mm, diameter of tube as 8 mm, and surrounding temperature at 10 °C. The values are calculated for $h = 0$ from Eq. (53), others from Eq. (44). The metal is gallium.

$$R_0(\beta_0, r) = 1 \tag{51}$$

$$\frac{1}{N(\beta_0)} = \frac{2}{R^2 - r_0^2} \tag{52}$$

Therefore, the final solution can be obtained as:

$$\begin{aligned}\theta(r,t) = {} & \left\{ \int_{r_0}^{R} \frac{2}{R^2 - r_0^2} r F(r) e^{-a\beta_m^2 t}\, dr \right. \\ & + \sum_{m=1}^{\infty} \left\{ \frac{[RJ_1(\beta_m R) + RY_1(\beta_m R)]e^{-a\beta_m^2 t}}{\beta_m N(\beta_m)} \right. \\ & \left. \left. - \frac{[r_0 J_1(\beta_m r_0) + r_0 Y_1(\beta_m r_0)]e^{-a\beta_m^2 t}}{\beta_m N(\beta_m)} \right\} \right. \\ & \left. \times F(r) R_0(\beta_m, r) \right\} - \left\{ \frac{\alpha\rho L}{k} \frac{t}{R^2 - r_0^2} \frac{R^2}{t_1} \right. \\ & \left. + \frac{\rho L}{2k} \sum_{m=1}^{\infty} \frac{R^2 R_0(\beta_m, s)(1 - e^{-a\beta_m^2 t})}{\beta_m^2 N(\beta_m) t_1} R_0(\beta_m, r) \right\} \\ & + \frac{\alpha Q}{\pi k} \frac{t}{R^2 - r_0^2} \\ & + \frac{Q}{2\pi k} \sum_{m=1}^{\infty} \frac{(1 - e^{-a\beta_m^2 t}) R_0(\beta_m, r_0)}{\beta_m^2 N(\beta_m)} R_0(\beta_m, r) \end{aligned} \tag{53}$$

The heat transfer coefficient of natural convection for air is at the order of 1 W/(m^2 K) and therefore we choose it as 5 W/(m^2 K) in above calculation. Different heat transfer coefficients are tried and the results are shown in Fig. 5. It was observed that, the time needed for thawing the metal increases slightly when heat transfer coefficient increases. There is no significant role for choosing the convective heat transfer coefficient when calculating the physical model exposing to the air. However, the forced convection of air may play significant role. For example, when choosing the parameters as follows: $r_0 =$ 0.2 mm, $R = 4$ mm, $k = 29.4$ W/(m K), $a = 1.83 \times 10^{-5}$ m^2/s, $Q = 100$ W/m, the time needed for thawing process is 253.6 second for the case of forced convective heat transfer with $h = 20$ W/(m^2 K), and 317.1 seconds for 100 W/(m^2 K).

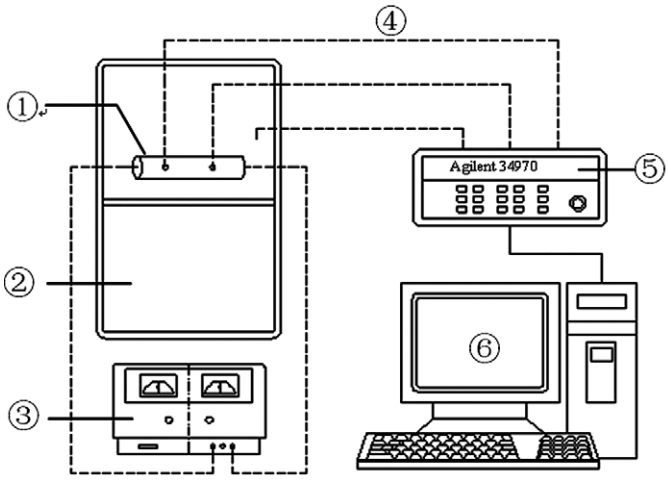

Fig. 6. Schematic illustration for the experimental system. (1) Experimental tube; (2) Refrigerator; (3) Power supply; (4) Thermocouples; (5) Data acquisition instrument; (6) Computer.

4.1.5. *Effect of thermal conductivity*

In the aforementioned theoretical analysis, we have assumed $k_s = k_l = k$, and chosen the liquid gallium's thermal conductivity, namely 29.4 W/(m K) in the calculation. However, the thermal conductivity of solid gallium is 40.6 W/(m K). Table 3 presents the time needed for thawing process when two different thermal conductivity values are chosen in the calculation. The calculated error values of time needed for thawing show that it is reasonable and acceptable when the thermal conductivity of liquid metal is considered as constant.

4.2. *Conceptual experiment*

4.2.1. *Description of experimental set-up*

For demonstrating the concept of using wire heater to quickly thaw the frozen low melting point metal, a schematic of the experimental setup is given in Fig. 6. A copper tube filled with gallium is tested in this paper, as shown in Fig. 7. The wall of the copper tube to hold the liquid metal is of small thickness for a good heat transfer with the environment. Because of high thermal conductivity and small thickness of the tube wall, the thermal resistance between the metal and the surrounding air is ignored, which is close to the analytical study. The low temperature atmosphere is realized by using the closet of a refrigerator.

Two holes are drilled in the tube wall to mount the thermocouples at $r = R$. Another thermocouple is used to test the environmental temperature. The data are recorded by the Agilent (USA) data acquisition system. As shown in Fig. 7(b), a direct power is supplied to heat the wire heater, whose electric resistance is 0.19 ohm. Because of electrical conductance, the nickel wire used as wire heat should be coated with insulating material. We assume the whole metal become thawed when the temperature point at the measured location climbs to the melting point.

Table 3
The time calculated from Eq. (44) for different thermal conductivity values, under condition of $h = 5$ W/(m^2 K), $r_0 = 0.2$ mm, and $R = 4$ mm

Input power of wire heater (W/m)	$k = 40.6$ W/(m K)	$k = 29.4$ W/(m K)	Mean value	Error
50	504.4	498.3	501.35	0.61%
75	334.7	330.6	332.65	0.62%
100	250.5	247.4	248.95	0.62%
125	200.1	197.7	198.9	0.6%
150	166.7	164.6	165.65	0.63%
175	142.8	141.0	141.9	0.63%
200	124.9	123.4	124.15	0.6%

Units: second.

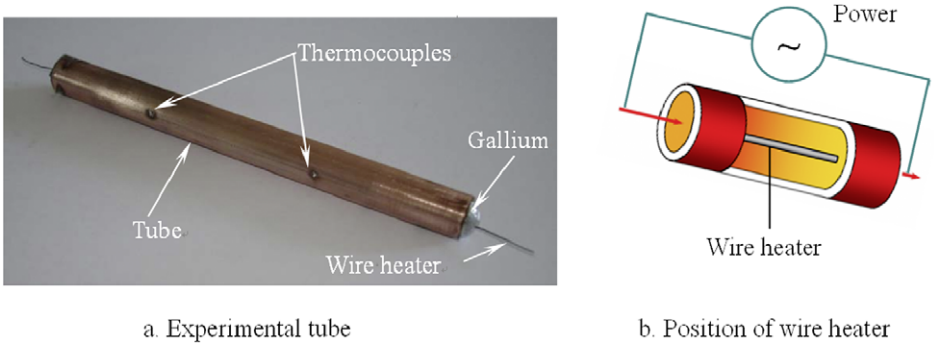

Fig. 7. The experimental tube with nickel wire as the central heater and gallium as the low melting metal.

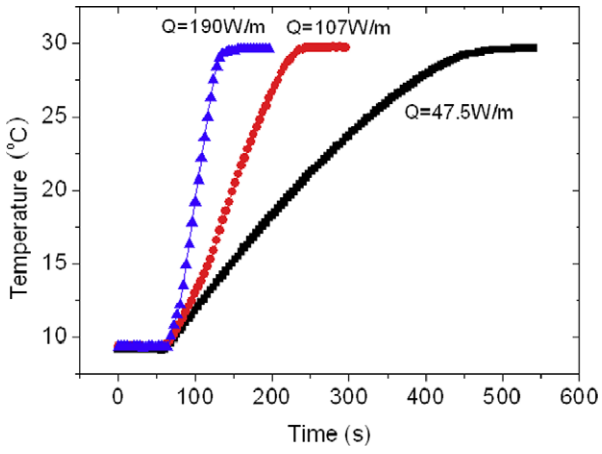

Fig. 8. The temperature at $r = R$ when the applied power of wire heater is 47.5, 107, and 190 W/m, respectively. Gallium's thermal properties are used in the calculation.

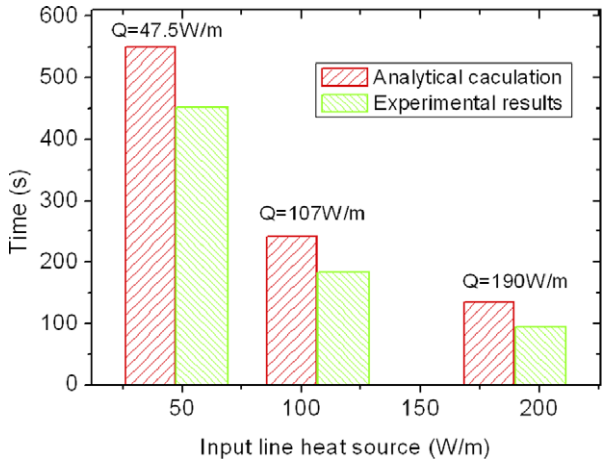

Fig. 9. Comparisons between analytical solution and experimental measurements on thawing gallium.

4.2.2. Measurement results

For the present analysis, typical low melting point metal gallium is considered. Its thermal properties are as follows [19]: $\rho = 5904$ kg/m^3, $a = 1.83 \times 10^{-5}$ m^2/s, $k = 29.4$ W/(m K). The heating wire is the nickel with diameter $r_0 = 0.0002$ m and length $L = 0.14$ m. The inner diameter of the tube is $R = 0.004$ m, which is also adopted in the experiments.

Fig. 8 depicts the transient temperature at $r = R$ when the power of the heating wire is 47.5, 107, and 190 W/m, respectively. Comparison between calculation based on corresponding parameters and experimental measurements are shown in Fig. 9.

Fig. 9 indicates that the experimental time for thawing the frozen gallium appears a little smaller than the analytical result, partly because the atmosphere temperature increases slightly while an additional energy is loaded which therefore speeds up the thawing of the metal gallium. Another reason may come from that one-dimensional approximation in the theoretical model may produce certain errors due to finite length of the experimental copper tube. In real application, the liquid metal loop may be longer than the length of experimental tube and has smaller diameter, close to 1-D model. The third reason may lie in the approximate treatment of ds/dt. Overall, the theory and measurements accord well with each other in an acceptable range.

From the above experiment, it has been demonstrated that the frozen gallium can be thawed successfully by a wire heater positioned in the center of the tube. This method is expected to

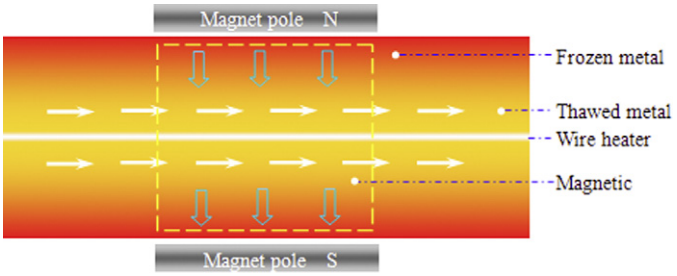

Fig. 10. The metal coolant begins to flow after being thawed under Lorentz's Force.

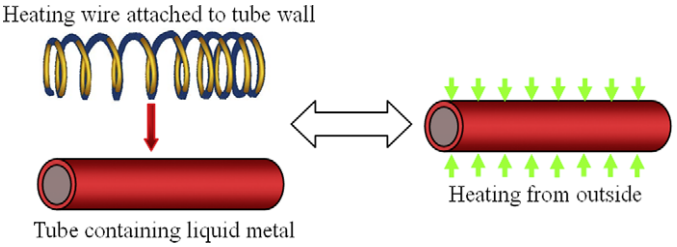

Fig. 11. A method of thawing frozen metal with heat flux from the outer wall of the tube.

find future application in liquid metal cooling in thermal management.

4.3. Discussion

4.3.1. Time needed for thawing metal driven by MHD pump

In a real application, such as liquid metal driven by a MHD pump, because of existence of magnetic field, the liquid metal began to flow immediately after it becomes thawed. That is to say, the liquid metal cooling loop will start to work after the wire heater is activated, which helps reduce the disadvantage for the low melting point metal to completely thaw. The solid-state metal can work as a tube with wall which becomes thinner and thinner with the time.

The present calculations are based on the properties of gallium because it is easily available. However, the method is applicable to various metals need thawing. Although the analytical studies deviate with the experimental results more or less, it can still predict the time needed for thawing. Furthermore, the methods can also be extended for analyzing the freezing process of the liquid metal running in the thermal management system.

4.3.2. Surface heating to thaw the frozen metal

The time needed for thawing the frozen metal through supplying heat from outer wall of the tube can also be obtained using the methods as developed in this paper. Fig. 11 shows one of the ways to apply heat flux at the copper tube.

For such approach of thawing the frozen metal, the energy conservation equations can be described as follows:

$$\frac{1}{\alpha}\frac{\partial\theta}{\partial t} = \left(\frac{\partial^2\theta}{\partial r^2} + \frac{1}{r}\frac{\partial\theta}{\partial r}\right) + \frac{q(r,t)}{k} \tag{54}$$

$$k\frac{\partial\theta}{\partial r} = q_0, \quad r = R \tag{55}$$

$$\theta(r,0) = F(r) = T_0(r) - T_f \tag{56}$$

where, $q(r,t) = -\rho L\frac{ds}{dt}\delta[r-(R-s(t))]$.

Using a similar separating variable method as performed in aforementioned sections, the Green's function to Eqs. (54)–(56) can be obtained as

$$G(r,t|r',\tau) = \frac{2}{R^2} + \sum_{m=1}^{\infty}\frac{1}{N(\beta_m)}e^{-a\beta_m^2(t-\tau)}R_0(\beta_m,r)R_0(\beta_m,r') \tag{57}$$

where, β_m's are the positive roots of

$$J_1(\beta_m R) = 0 \tag{58}$$

with eigenfunctions $R_0(\beta_m, r)$ and the norm $N(\beta_m)$ as

$$R_0(\beta_m,r) = J_0(\beta_m r) \tag{59}$$

$$N(\beta_m) = \frac{R^2 J_0^2(\beta_m R)}{2} \tag{60}$$

It needs to be noted that $\beta_m = 0$ is also an eigenvalue with corresponding eigenfunction and norm as $R_0(\beta_m, r) = 1$ and $N(\beta_0) = R^2/2$.

According to the Green's function, the solution to Eqs. (54)–(56) are as follows

$$\begin{aligned}\theta(r,t) = {} & \int_0^R r'G(r,t|r',\tau)|_{\tau=0}F(r')\,dr' \\ & + \frac{\alpha}{k}\int_0^t d\tau\int_0^R r'G(r,t|r',\tau)q(r',\tau)\,dr' \\ & + \alpha\int_0^t r'G(r,t|r',\tau)\frac{1}{k}f_{r'}(r,t)|_{r'=R}\,d\tau\end{aligned} \tag{61}$$

where, $f_R(r,t) = q_0$.

Considering $q(r,t) = -\rho L\frac{\partial s}{\partial t}\delta[r-(R-s(t))]$, Eq. (61) can be rewritten as

$$\begin{aligned}\theta(r,t) = {} & \frac{2}{R^2}\int_a^b r'F(r')\,dr' + \sum_{m=1}^{\infty}\frac{2}{R^2J_0^2(\beta_m R)}e^{-a\beta_m^2 t}J_0(\beta_m r) \\ & \times\int_0^R r'J_0(\beta_m r')F(r')\,dr' - \frac{\alpha\rho L}{k}\frac{2}{R^2}\big(R-s(t)\big) \\ & \times\left\{t - \sum_{m=1}^{\infty}\frac{2}{R^2a\beta_m^2J_0^2(\beta_m R)}J_0(\beta_m r)\right. \\ & \left.\times J_0\big(\beta_m\big(R-s(t)\big)\big)\big(1-e^{-a\beta_m^2 t}\big)\right\}\frac{ds}{d\tau} \\ & + \frac{2\alpha q_0}{kR}\left(t + \sum_{m=1}^{\infty}\frac{1}{a\beta_m^2J_0^2(\beta_m R)}J_0(\beta_m r)J_0(\beta_m R)\right. \\ & \left.\times\big(1-e^{-a\beta_m^2 t}\big)\right)\end{aligned} \tag{62}$$

Similar methods as discussed before can be applied to treat ds/dt, we assume

$$\frac{d(R-s)}{d\tau} = \frac{A}{R-s} \tag{63}$$

One can then get $A = R^2/2t_1$ when introducing similar expressions in Eqs. (39)–(41). Therefore, we have

$$\frac{d(R-s)}{d\tau} = \frac{R^2}{2t_1(R-s)} \tag{64}$$

namely,

$$\frac{ds}{d\tau} = -\frac{R^2}{2t_1(R-s)} \tag{65}$$

The solution to Eq. (62) can finally be obtained as

$$\begin{aligned}\theta(r,t) = {} & \frac{2}{R^2}\int_a^b r' F(r')\,dr' + \sum_{m=1}^{\infty} \frac{2}{R^2 J_0^2(\beta_m R)} e^{-a\beta_m^2 t} J_0(\beta_m r) \\ & \times \int_0^R r' J_0(\beta_m r') F(r')\,dr' \\ & + \frac{\alpha\rho L}{kt_1}\left\{ t - \sum_{m=1}^{\infty} \frac{2}{R^2 a\beta_m^2 J_0^2(\beta_m R)} \right. \\ & \left. \times J_0(\beta_m r) J_0\big(\beta_m R(t/t_1)^{1/2}\big)\big(1 - e^{-a\beta_m^2 t}\big) \right\} \\ & + \frac{2\alpha q_0}{kR}\left(t + \sum_{m=1}^{\infty} \frac{1}{a\beta_m^2 J_0^2(\beta_m R)} J_0(\beta_m r) J_0(\beta_m R) \right. \\ & \left. \times \big(1 - e^{-a\beta_m^2 t}\big) \right)\end{aligned} \tag{66}$$

4.3.3. Thawing of frozen metal through both surface heating and wire heating

Except for using only a central wire heater to thaw the frozen metal, a heat flux can also be applied simultaneously from the wall of the outer tube. This would further shorten the time requested for thawing the metal. Protocol for such case can also find application in reality.

To analytically address this issue, one can assume the heat flux as constant q_0, i.e. in Eq. (34), $f_R(r,t) = q_0$. Considering the heat transfer coefficient $h = 0$, the temperature distribution can be obtained easily from Eqs. (44) and (53):

$$\begin{aligned}\theta(r,t) = {} & \left\{ \int_{r_0}^{R} \frac{2}{R^2 - r_0^2} r F(r) e^{-a\beta_m^2 t}\,dr \right. \\ & + \sum_{m=1}^{\infty} \left\{ \frac{[RJ_1(\beta_m R) + RY_1(\beta_m R)]e^{-a\beta_m^2 t}}{\beta_m N(\beta_m)} \right. \\ & \left. \left. - \frac{[r_0 J_1(\beta_m r_0) + r_0 Y_1(\beta_m r_0)]e^{-a\beta_m^2 t}}{\beta_m N(\beta_m)} \right\} F(r) R_0(\beta_m, r) \right\} \\ & - \left\{ \frac{2\alpha\rho L}{k} \frac{st}{R^2 - r_0^2} \frac{ds}{dt} \right. \\ & + \frac{\rho L}{k} \sum_{m=1}^{\infty} \frac{s R_0(\beta_m, s)(1 - e^{-a\beta_m^2 t})}{\beta_m^2 N(\beta_m)} \frac{ds}{dt} R_0(\beta_m, r) \Bigg\} \\ & + \left\{ \frac{\alpha Q}{\pi k} \frac{t}{R^2 - r_0^2} \right. \\ & + \frac{Q}{2\pi k} \sum_{m=1}^{\infty} \frac{(1 - e^{-a\beta_m^2 t}) R_0(\beta_m, r_0)}{\beta_m^2 N(\beta_m)} R_0(\beta_m, r) \\ & \left. + \frac{Rq_0}{k} \sum_{m=1}^{\infty} \frac{(1 - e^{-a\beta_m^2 t}) R_0(\beta_m, R)}{\beta_m^2 N(\beta_m)} R_0(\beta_m, r) \right\}\end{aligned} \tag{67}$$

In this relation, the value of ds/dt needs further study due to unknown position of solid–liquid interface, which was decided by the value of wire heater as well as the heat flux at $r = R$.

5. Conclusion

In this study, a novel strategy to thaw the frozen low-melting metal is successfully demonstrated. It involves a wire heater centered longitudinally in a tube. The physical model was established with moving heat source method and solved analytically using Green' function. The calculations agree fundamentally well with the experimental measurements. Both results show the high efficiency of the heating approach in quickly thaw the frozen metal for thermal management. While dealing with solid–liquid interface velocity in moving boundary problem, a feasible way to treat the velocity was also proposed for finite cylindrical zone. The methods as established in the present paper are expected to be useful in future research in this area.

Acknowledgements

This work is partially supported by the National Natural Science Foundation of China under Grants of 50575219 and 50576103.

References

[1] J. Liu, Y.X. Zhou, A computer chip cooling method which uses low melting point metal and its alloys as the cooling fluid, China Patent: 02131419.5, 2002.
[2] A. Miner, U. Ghoshal, Cooling of high-power-density microdevices using liquid metal coolants, Appl. Phys. Lett. 85 (2004) 506.
[3] I. Silverman, A.L. Yarin, S.N. Reznik, A. Arenshtam, D. Kijet, A. Nagler, High heat-flux accelerator targets: Cooling with liquid metal jet impingement, Int. J. Heat Mass Trans. 49 (2006) 2782–2792.
[4] O. Andreev, Y. Kolesnikov, A. Thess, Experimental study of liquid metal channel flow under the influence of a nonuniform magnetic field, Phys. Fluids 18 (2006) 065108.
[5] K. Mohseni, E.S. Baird, Digitized heat transfer using electrowetting on dielectric, Nanoscale and Microscale Thermophysical Engineering 11 (2007) 99–108.
[6] E.S. Baird, K. Mohseni, Digitized heat transfer: A new paradigm for thermal management of compact micro systems, IEEE Transactions on Components and Packaging Technologies 31 (2008) 143–151.
[7] K.Q. Ma, J. Liu, Heat-driven liquid metal cooling device for the thermal management of computer chip, J. Phys. D: Appl. Phys. 40 (2007) 4722–4729.
[8] V. Singhal, S.V. Garimella, Induction electrohydrodynamics micropump for high heat flux cooling, Sensor Actuat. A Phys. 134 (2007) 650–659.

[9] K. Mohseni, Effective cooling of integrated circuits using liquid alloy electrowetting, in: 21st IEEE SEMI-THERM Symposium, 2005.

[10] C.G. Cooney, C.Y. Chen, M.R. Emerling, A. Nadim, J.D. Sterling, Electrowetting droplet microfluidics on a single planar surface, Microfluid Nanofluid 2 (2006) 435–446.

[11] T. Li, Y.G. Lv, J. Liu, Y.X. Zhou, A powerful way of cooling computer chip using liquid metal with low melting point as the cooling fluid, Forsch Ingenieurwes 70 (2005) 243–251.

[12] K.Q. Ma, J. Liu, Nano liquid-metal fluid as ultimate coolant, Phys. Lett. A 361 (2007) 252–256.

[13] Y.L. Gao, W.B. Guan, Q.J. Zhai, K.D. Xu, Study on undercooling of metal droplet in rapid solidification, Sci. China Ser. E 48 (2005) 632–637.

[14] K.Q. Ma, J. Liu, Liquid metal cooling in thermal management of computer chip, Front. Energy Power Eng. China 1 (2007) 384–402.

[15] M.N. Ozisik, Heat Conduction, second ed., Wiley, 1993.

[16] J. Liu, Y.X. Zhou, Analytical study on the freezing and thawing processes of biological skin with finite thickness, Heat Mass Trans. 38 (2002) 319–326.

[17] C.Y. Yang, The determination of two moving heat sources in two-dimensional inverse heat problem, Appl. Math. Model. 30 (2006) 278–292.

[18] Y.M. Ali, L.C. Zhang, Relativistic moving heat source, Int. J. Heat Mass Trans. 48 (2005) 2741–2758.

[19] Z.Y. Qian, Thermophysical Properties of Low Melting Point Metal, Science Press, Beijing, 1985.